

# Grating interferometer for flatness testing

Peter J. de Groot

Zygo Corporation, Laurel Brook Road, Middlefield, Connecticut 06455

Received June 26, 1995

Two diffraction gratings placed in front of a flat surface generate an interference pattern representing the surface deformations. The interference pattern is achromatic and has an equivalent wavelength between 4 and 40  $\mu\text{m}$ , depending on the grating frequencies and the viewing angle. Using phase-shifting techniques, the grating interferometer provides high-precision profile measurements of both smooth and rough surfaces.  
© 1996 Optical Society of America

Optical metrology can generally be divided into two regimes, interferometric and geometric. Interferometry relies on the wave nature of light and is represented by a range of techniques and commercial products, including the now-ubiquitous phase-shifting Fizeau interferometer. Geometric techniques include triangulation and moiré interferometry. The advantage of interferometry is high accuracy, of the order of a few nanometers for surface testing, whereas geometric metrology is much more forgiving of surface roughness and deformations. Interferometry is best for lenses and mirrors, and geometric optics is best for machined metal parts. The current state of the art provides little overlap between the two techniques.

The grating interferometer described in this Letter is an attempt to bridge the gap between interferometric and geometric optical metrology in flatness testing. The proposed instrument uses a pair of phase-diffraction gratings to illuminate an object with two beams at different angles of incidence. The same pair of gratings recombines the two beams, resulting in an interference pattern with an equivalent wavelength approximately ten times larger than the optical wavelength of the illuminating light. The scale of the measurement is therefore situated between conventional interferometry and geometric techniques such as moiré interferometry.

Figure 1 shows the light paths through the gratings. Collimated source light illuminates grating G1 and diffracts into two first-order beams, A and B. Grating G2, which has a grating frequency twice that of G1, redirects beams A and B so that they combine on the object surface. The reflected light from the surface passes back through the gratings and interferes on the CCD camera array. The sensitivity of the grating interferometer to surface deformation is caused by the difference in the incident angles  $\alpha$  and  $\beta$  of beams A and B on the object surface. The interference equation for two beams incident at different angles is

$$g = g_0 + Vg_0 \cos(2\pi z/\Lambda), \quad (1)$$

where  $z$  is the surface height,  $g_0$  and  $V$  are constants, and

$$\Lambda = \frac{\lambda}{\cos(\beta) - \cos(\alpha)} \quad (2)$$

is an equivalent wavelength.<sup>1,2</sup> With a suitable choice of angles  $\alpha$  and  $\beta$  almost any equivalent wavelength is possible.

An unusual characteristic of the grating interferometer in Fig. 1 is that angles  $\alpha$  and  $\beta$  are governed by the diffractive properties of the grating pair. The angles can be related to the incident angle  $\gamma$  of the source beam with respect to G1:

$$\sin(\alpha) = \sin(\gamma) + N_1\lambda, \quad (3)$$

$$\sin(\beta) = \sin(\gamma) - N_1\lambda, \quad (4)$$

where  $N_1$  and  $N_2$  are the grating frequencies of G1 and G2, respectively. Using the small-angle approximation

$$\cos(\alpha) \approx 1 - \frac{1}{2} \sin^2(\alpha), \quad (5)$$

we see that the equation for the equivalent wavelength reduces to

$$\Lambda \approx \frac{1}{2N_1 \sin(\gamma)}. \quad (6)$$

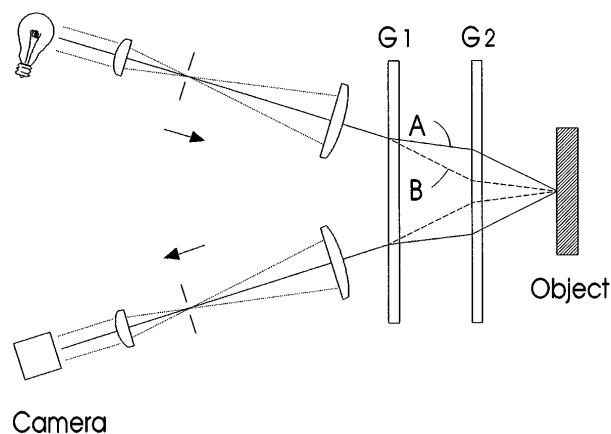


Fig. 1. Grating interferometer for flatness testing. G1 diffracts the source light into two beams, A and B, and G2 brings them back together again at the object surface. The sensitivity of the interferometer to surface deformation is caused by the difference in the incident angles of beams A and B on the object surface.

The equivalent wavelength of the interference fringes is independent of the source wavelength  $\lambda$ . The interference pattern is achromatic and is not limited by the temporal coherence properties of the source light.

Achromatic fringe formation is characteristic of moiré interferometry, which is generally interpreted geometrically. It is possible to analyze the properties of the interferometer shown in Fig. 1 in the same way. The key to the geometric interpretation is the notion that grating G2 creates an achromatic image of grating G1 on the object surface. The production of a fine-grain achromatic line pattern with a grating pair was studied extensively by Chang *et al.*<sup>3</sup> Viewed from this perspective, grating G2 may be thought of as a very high-numerical-aperture lens with conjugates at G1 and the object plane. The interpretation of the resulting interference pattern in the image plane is indeed similar to that of projection moiré with an unusually fine-pitch grating.

Whatever the physical interpretation of the interference phenomenon, the grating interferometer in Fig. 1 has considerable practical merit. The equivalent wavelength  $\Lambda$  for most practical combinations of gratings ranges from 4 to 40  $\mu\text{m}$ , so the instrument sensitivity is intermediate between visible-wavelength interferometry and geometric optics. The slope tolerance and the acceptable surface roughness are correspondingly increased with respect to conventional interferometry. The fringe contrast is excellent since both of the interfering beams reflect off the object, and the intensity balance is nearly independent of the surface reflectivity. Because the fringes are achromatic the source-wavelength stability is irrelevant, and conventional incandescent sources generate clear colorless fringes. The insensitivity to source wavelength is also a benefit when one is using laser-diode sources, which tend to be unstable spectrally.

Figure 2 shows experimental phase data for a grating interferometer having an equivalent wavelength  $\Lambda$  of 8  $\mu\text{m}$ . The object surface shown in Fig. 2 is a 30-mm-diameter portion of a sheet of brush-finished aluminum having a rms surface roughness of 0.4  $\mu\text{m}$ . The gratings for this interferometer are 75 nm in diameter, the frequency  $N_1$  is 300 grooves/mm, and the incident angle  $\gamma$  is 11.6°. The fringe analysis uses phase-shifting interferometry, in which a 256  $\times$  256 camera records a sequence of data frames during a linear phase shift of the interference pattern.<sup>4</sup> The phase shift is generated by a mechanical translator operating on G1, with a range of motion of the order of the equivalent wavelength  $\Lambda$ . The rms repeatability of the surface topography map shown in Fig. 3 is  $\Lambda/100$ .

The closest relative to the interferometer shown in Fig. 1 is the single-grating instrument of Jaerisch and Makosch.<sup>5</sup> In the single-element geometry the two interfering beams are two diffractive orders of the same grating. Other versions of the same concept include the flatness reference plate of Yeskov *et al.*<sup>6</sup> and the historical research of Barus.<sup>1</sup> One of the more inventive examples of a diffractive interferometer with a long equivalent wavelength is the holographic system devised by Boone and Jacquot, which combines

the amplitude-division properties of gratings with the focusing power of spherical holograms in a remarkably simple and effective instrument.<sup>7</sup> However, all these single-element methods require that the grating be nearly in contact with the object surface, to minimize wave-front shear and balance the path differences. They also do not have the achromatic fringe formation that is characteristic of the double-grating geometry shown in Fig. 1.

The two-grating geometry has its own complications arising from the need to control the multiple diffractive orders. The ideal gratings G1 and G2 should have suppressed zero-order transmission and should be free of any surface defects. Although these requirements are not always easily achieved in practice, the proposed grating interferometer enjoys a combination of advantages ideal for bridging the gap between interferometric and geometric metrology. It has a large working distance, it can accommodate a variety of light sources, and it is relatively insensitive to vibration compared with conventional interferometers. The interference pattern has high contrast, even with rough

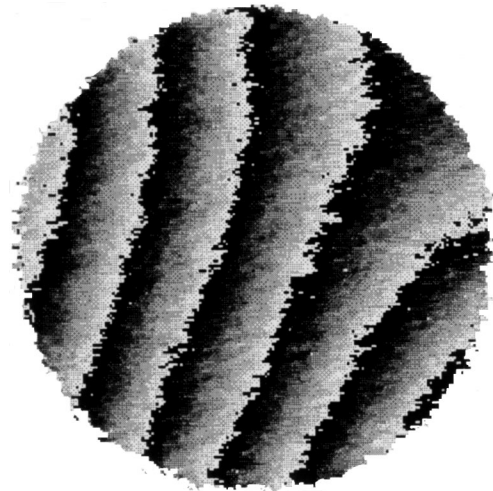


Fig. 2. Wrapped phase map for a 30-mm-diameter portion of a brush-finished aluminum disk. The 0.4- $\mu\text{m}$  rms surface roughness is too large for conventional visible-wavelength interferometers.

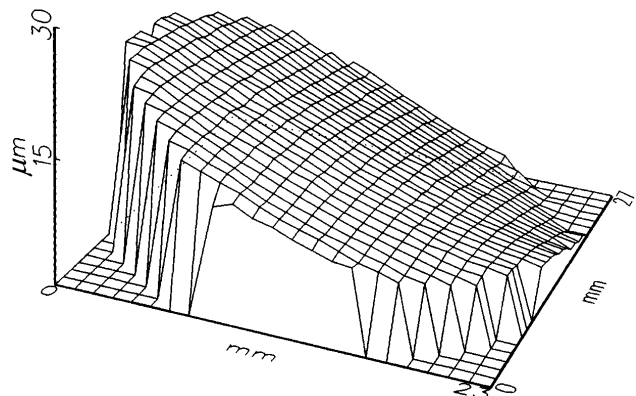


Fig. 3. Processed surface topography data generated from the phase map in Fig. 2. The rms measurement repeatability is 80 nm.

surfaces and objects with large slope errors. Phase-shifting techniques provide excellent measurement repeatability, and the equivalent wavelength is a good compromise between measurement range and the increasing demands of precision metrology in manufacturing.

### References

1. C. Barus, Carnegie Inst. Washington Publ. **149**, Pt. 1, Chap. 11 (1911).
2. F. H. Smith, U.S. patent 3,958,884 (April 16, 1976).
3. B. J. Chang, R. Alferness, and E. N. Leith, Appl. Opt. **14**, 1592 (1975).
4. J. E. Greivenkamp and J. H. Bruning, in *Optical Shop Testing*, D. Malacara, ed. (Wiley, New York, 1992), Chap. 14.
5. W. Jaerisch and G. Makosch, Appl. Opt. **12**, 1552 (1973).
6. D. N. Yeskov, S. N. Koreshev, and A. G. Seregin, Proc. SPIE **2340**, 461 (1994).
7. P. M. Boone and P. Jacquot, Proc. SPIE **1554A**, 512 (1991).